

Surfactant-mediated growth of Cu on Co(0001) investigated using medium-energy ion scattering

T. C. Q. Noakes* and P. Bailey

CCLRC Daresbury Laboratory, Daresbury, Warrington, WA4 4AD, United Kingdom

D. T. Dekadjevi and M. A. Howson

Department of Physics, University of Leeds, Leeds, LS2 9JT, United Kingdom

(Received 25 April 2003; published 27 October 2003)

Experiments were carried out using medium energy ion scattering (MEIS) to compare the structural properties of Cu films deposited on Co(0001) both with and without surfactant and before and after annealing to 300 °C. Films of 10-ML thickness were deposited onto the clean Co surface and onto a surface pre-dosed with 1 ML of Pb surfactant. MEIS data revealed a twinned fcc structure in all the deposited films irrespective of the presence of surfactant or the use of post deposition annealing. In the case of the Pb deposited surfaces the majority of surfactant was seen to float on the surface during growth but with a small quantity becoming distributed throughout the film. In addition to allowing 1-2 extra monolayers to grow epitaxially, the MEIS data provided evidence of improved crystallinity for films grown with the surfactant. Annealing the sample to 300 °C appeared to have little or no effect on the deposited films.

DOI: 10.1103/PhysRevB.68.155425

PACS number(s): 68.55.Jk, 68.35.-p, 68.49.-h

I. INTRODUCTION

The epitaxial growth of Cu on Co is of interest due to the importance of this material system in giant magnetoresistance (GMR) films.^{1,2} The magnetic properties of thin films are inextricably linked to their structure and hence considerable effort has gone into understanding and improving the growth.

Previous work on this system has shown that using a Pb surfactant during the growth of the multilayers can lead to enhanced GMR properties.³ In another study,⁴ the enhanced magnetic properties obtained using Pb surfactant mediated growth were shown to be linked with improved structural homogeneity in the layers. The benefits claimed for surfactant mediated epitaxy (SME) included enhanced layer-by-layer growth for Co, fcc structure in the Co layers, and suppression of twinning in the Cu layers.

Several studies of the growth of Co on Cu(111) have been conducted, including one using the technique of medium energy ion scattering (MEIS) (Ref. 5) which indicated pseudomorphic fcc growth for thin layers with the Co reverting to its natural hcp structure at increased film thickness. This behavior has also been observed in other studies,^{6,7} although there is some debate over the film thickness at which the fcc to hcp transition occurs. Compared to the growth of Co on Cu(111), Cu growth on Co(0001) has received relatively little attention, perhaps because of the difficulty involved in preparing clean, well ordered Co substrates. The major exception to this is a low-energy electron diffraction study of the early stages of epitaxial growth of Cu on Co(0001).⁸ Layer-by-layer growth was observed up to 4 ML and, interestingly, Cu overgrowth was seen to give rise to stacking faults in the Co such that the near surface region became fcc. No previous study of the effect of surfactant on this growth system has been conducted.

The most comparable work on surfactant mediated growth are the studies carried out on the homoepitaxial growth of Cu on Cu(111).^{9,10} Growth without a surfactant

was seen to give rise to two-domain growth and considerable islanding of the deposited film as a direct result of two features of the fcc(111) surface, the presence of two threefold adsorption sites and the high value of the Ehrlich-Schwoebel barrier which effectively suppresses interlayer diffusion.⁸ The use of a monolayer of Pb as a surfactant for the growth was seen to promote layer-by-layer growth by modifying the diffusion mechanism such that the preference between interlayer and intralayer mass transport changes.⁹

II. EXPERIMENT

The MEIS technique can obtain both structural and compositional information as a function of depth in the near surface region from the following effects. Compositional information can be obtained from the energy loss of elastically scattered ions. Structural information is provided by the angular variation of scattered ion intensity due to the phenomena of channelling and blocking which are seen when one atom casts a shadow on another directly behind it either in the incoming or scattered ion direction. Depth sensitivity comes from the inelastic energy loss of the ions as they travel through the sample.

The experiments were carried out at the Daresbury Laboratory MEIS facility (described elsewhere¹¹) using 100-keV He⁺ ions. Scattered ion intensity was measured with a toroidal electrostatic analyzer and position sensitive detector that allows the simultaneous measurement of scattered ion intensity over a range of energies and angles. A series of these two-dimensional scans have been electronically pasted together to form the full data set presented in Fig. 1 where the ion intensity is represented by a false color scale. These two-dimensional data sets can be further processed by integration of selected regions in either energy or angle to form more conventional one-dimensional plots with the energy spectra providing compositional information and the angular spectra providing structural information. Another type of spectrum presented in this work is obtained by monitoring the intensity

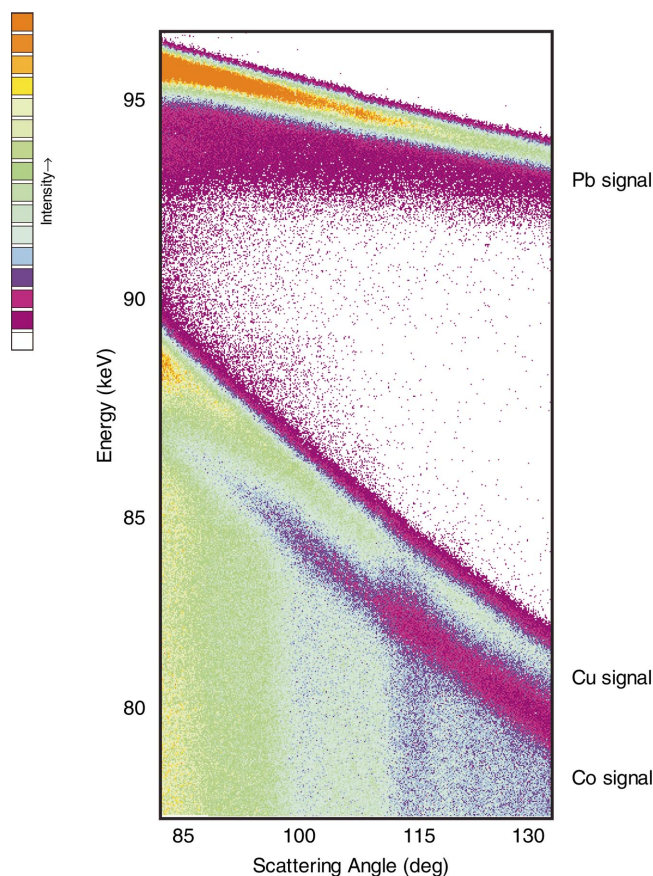


FIG. 1. (Color) Two-dimensional data set with intensity represented as a false color scale from a 10 ML Cu film grown on a Co(0001) substrate in the presence of a ML of Pb surfactant. The three elemental species are well separated in energy. Compositional data can be obtained from energy plots resulting from one-dimensional cuts through the data set. Conversely, by projecting the data onto the angle axis, blocking spectra can be produced which contain information on the structure.

from a defined area of the two-dimensional array (often the whole area) at fixed incidence angle (normally corresponding to a known channeling direction) while varying the azimuthal orientation of the sample. Scans of this type provide information on the periodicity of the sample and by selecting the appropriate scattering angle and energy different elements and depth regions can be probed.

The Co(0001) sample was prepared by repeated cycles of 1-kV Ar^+ ion bombardment and annealing to 400 °C (limited by the hcp to fcc phase transition at 422 °C). In addition, annealing for 5 min at 280 °C in 10^{-7} -mbar O_2 was also employed to reduce the level of residual C to below the detection limit of Auger electron spectroscopy (AES). After cleaning low energy electron diffraction (LEED) showed a clear sixfold pattern indicative of a clean, well ordered (1×1) surface. Deposition of Cu onto the room temperature sample was carried out using a hot filament source with the growth monitored using a quartz crystal microbalance to ensure a constant thickness for all the experiments. Pb surfactant deposition was carried out using a miniature *K*-cell that

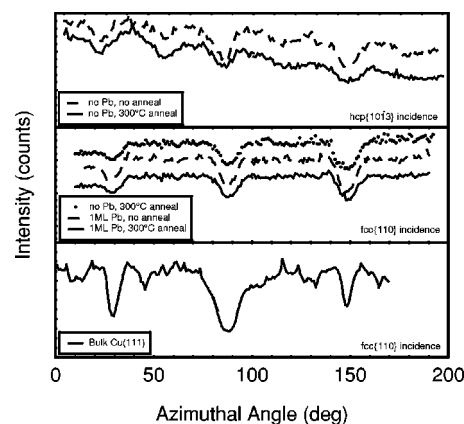


FIG. 2. Azimuthal scan data from a single crystal Cu(111) sample and Cu overlayers grown on Co(0001). The thin film data has been taken in two incidence directions, the fcc{110} and the hcp{10 $\bar{1}$ 3}. Sixfold symmetry can be observed for all the thin film data indicating either a hcp or more likely a twinned fcc structure.

had been previously calibrated to give a 0.1-ML/min rate, thus allowing 1 ML to be accurately obtained.

III. RESULTS

A. Azimuthal scans

Azimuthal scan data from the as deposited and annealed Cu films are presented in Fig. 2. In the case of the films deposited with no surfactant azimuthal scans have been collected with the beam incident along a {10 $\bar{1}$ 3} channel of the hcp Co bulk. For the annealed sample and those films grown with a surfactant the scans have been collected using alignment in a {110} direction in the Cu overlayer. For a perfect fcc crystal the incidence angle should be 35.3° from the surface normal, however for the theoretical maximum strain level expected for epitaxially grown Cu on Co this angle could reduce to 33.7° which is closer to the 32.0° expected for the hcp {10-13} channel. A previously measured {110} azimuthal scan from the bulk of a Cu(111) crystal is also included in the figure for comparison. While the bulk Cu signal clearly shows threefold periodicity all the Cu thin film data, independent of growth conditions, have sixfold symmetry indicating either hcp, or more likely twinned fcc growth. This data shows that the use of a Pb surfactant has not suppressed twin formation in the grown layers. However, closer inspection of the amplitudes of the channels seen in Fig. 2 reveals some interesting indications of a possible effect of the surfactant. Table I contains amplitude data for each of the azimuthal scans from the grown thin films, and there is a clear indication that the Pb grown layers have deeper channels than those grown without the surfactant indicating improved crystalline quality. However, comparing the data before and after annealing for samples grown both with and without surfactant, shows that the post annealing had no noticeable effect on the structure of the films.

B. 2D data

Figure 1 contains raw two-dimensional (2D) data from the surfactant grown sample after annealing. Co, Cu and Pb sig-

TABLE I. Comparison of the amplitudes of channelling dips in the azimuthal spectra presented in Fig. 2. The films grown with the Pb surfactant appear to have an improved crystallinity, although annealing the films to 300 °C had no apparent effect.

	fcc{110} channelling	hcp{10 $\bar{1}$ 3} channelling
Cu on Co(0001), no Pb. no anneal		72%/72%
Cu on Co(0001), no Pb. 300 °C anneal	69%/76%	68%/74%
Cu on Co(0001), 1-ML Pb. no anneal	59%/52%	
Cu on Co(0001), 1-ML Pb. 300 °C	53%/59%	

nals can be seen to be clearly resolved. Spectra of this type are further processed to produce the 1D energy or angle spectra presented in the following sections.

1. Energy spectra

Figure 3 contains energy spectra projected from 2D data taken from films grown both with and without surfactant after annealing. The preannealing data (not shown) was very similar, again indicating that the 300 °C anneal had no effect. The data has been fitted using the SIMNRA package¹² to determine the composition and thicknesses of the deposited materials. For both samples the amount of deposited Cu is 6×10^{16} atoms/cm², which equates to 10 ML. The surfactant grown layer has the equivalent of 1 ML of Pb residing at the surface but in addition, there is clearly some subsurface Pb also present. One possibility considered for this subsurface signal was Pb atoms trapped at the interface between the Co surface and the Cu layer. However, this was discounted since modeling showed that the signals from the surface and subsurface Pb should be resolved in energy, which is inconsistent with the data. In order to account for all of the observed signal, residual Pb must be distributed throughout the grown

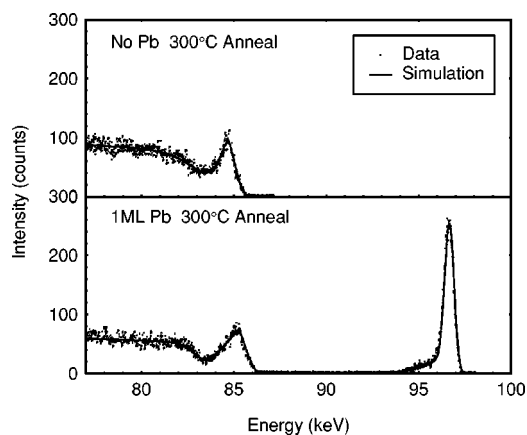


FIG. 3. Energy spectra derived from two-dimensional data sets for 10-ML Cu thin films grown on Co(0001) both with and without surfactant after annealing to 300 °C. Fits produced using the SIMNRA simulation code are also presented.

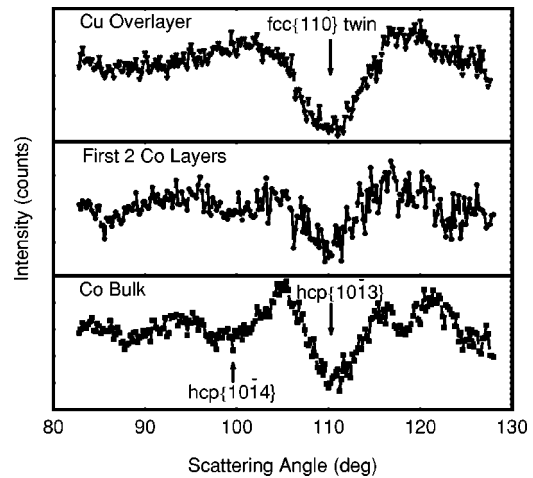


FIG. 4. Blocking spectra obtained from a 10 ML Cu film grown on Co(0001) with 1 ML after annealing to 300 °C. The projections have been obtained at different energies to probe the structure in the Co bulk, Co top two layers, and Cu overlayer.

layer at a constant level of approximately 5%. The simulation produced for this compositional structure gives excellent agreement with the data as seen in Fig. 3. An additional parameter seen to improve the fits was the roughness or variation in thickness of the deposited film. Although the absolute values of roughness parameter generated have limited validity under the experimental conditions used, it was interesting to note that the value for the Pb assisted sample was less than its non-surfactant grown counterpart suggesting a more uniform film thickness.

2. Angular spectra

Figure 4 contains angular spectra for the Co bulk, the top two layers of Co and the Cu overlayer for a sample prepared using surfactant after the 300 °C anneal. Data taken from the other grown films looked visually similar to this data but with subtle differences in terms of the amplitudes and angular positions of the blocking features. The Cu overlayer data shows one large blocking feature close to 110°. This scattering angle is consistent with a $\langle 110 \rangle$ -type direction in a twinned fcc crystal where this feature dominates because of the increased illumination in the opposing twin to that in which the incident beam is aligned. Other smaller features, which might be expected for both twinned components, may be damped by the disorder that would be expected in an imperfectly grown layer. In contrast to the overlayer, the Co bulk exhibits two features, namely, the hcp $\langle 10\bar{1}3 \rangle$ and hcp $\langle 10\bar{1}4 \rangle$ blocking dips. The signal from the first two layers of the Co substrate exhibits two similarly positioned features, which, at least superficially, resemble the hcp substrate more closely than the fcc overlayer.

A further aspect of the overlayer signal is that the $\langle 110 \rangle$ blocking dip does not occur at the precise angle expected for a perfect fcc crystal but rather exhibits a shift that is consistent with strain in the grown layer. By sectioning the overlayer signal in a monolayer-by-monolayer fashion and measuring the position of this dip it is possible to produce a strain profile of the deposited thin film [a methodology pre-

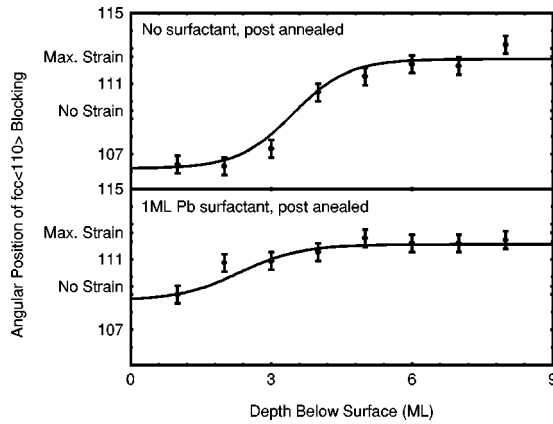


FIG. 5. Layer-by-layer strain profiles of the Cu overlayer signal for films grown both with and without surfactant after annealing to 300 °C. The profiles have models superimposed that show the expected behavior for abrupt transitions from strained to unstrained growth after 6 ML for the nonsurfactant sample and 7 ML for the Pb grown sample.

viously used in experiments on Au thin films on Cu(111) (Ref. 13)]. Figure 5 contains the results of such analysis for the annealed samples grown both with and without Pb surfactant. In addition, curves modeling the strain behavior have been included using a prediction of the actual strain, which has subsequently been smoothed using a three-point average to simulate the effect of the energy resolution of the analyzer on the depth resolution. In the case of the nonsurfactant grown layer the highest strain is 5.6% (95% of the theoretical maximum) with six layers growing epitaxially before an abrupt transition to a large (>10%) surface contraction. For the surfactant-grown sample the highest strain is 4.5%, which abruptly falls to a small surface contraction (2.7%) but with the transition delayed such that some 7–8 layers grow epitaxially.

In Fig. 3 residual Pb was seen to be present in the surfactant grown thin Cu film. The question remains as to where the lead is situated, either in or out of lattice sites. Figure 6 shows a comparison of angular spectra obtained from both the buried lead and the Cu overlayer for the annealed surfactant grown layer. The signal from the buried Pb shows an identical blocking pattern to the Cu in the thin film and for comparison the amplitude of the $\langle 110 \rangle$ twin blocking dip is $71 \pm 1\%$ for the Cu and $74 \pm 6\%$ for the Pb indicating a very similar crystallographic environment for the two atomic species.¹⁴

IV. DISCUSSION

Both the azimuthal and blocking pattern spectra are consistent with the growth of Cu on the Co substrate resulting in a twinned fcc overlayer. This conclusion has been confirmed by comparison of the blocking spectra from the overlayer with VEGAS simulations¹⁵ of twinned fcc structure for both nonsurfactant and surfactant grown films (Fig. 7). In fact, the formation of twins is to be expected since, if the clean surface exhibits monolayer steps, two domains of fcc would result even when the growth on individual terraces was

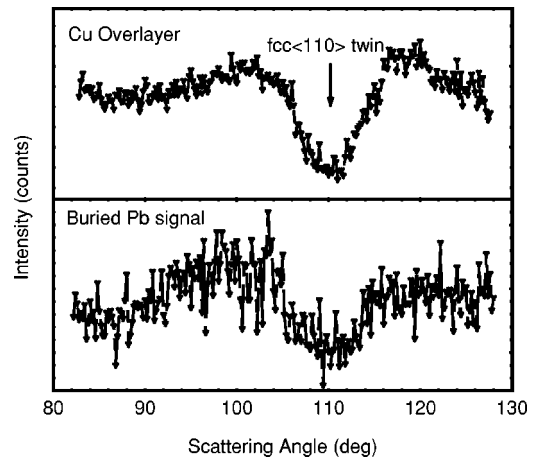


FIG. 6. Comparison of the blocking spectra for subsurface for the Cu overlayer and subsurface Pb, for the surfactant grown sample after annealing. The amplitudes of the fcc{110} twin blocking dip are similar in both cases.

single domain. In this sense the growth is not analogous to the case where Cu is grown on a thin Co layer above a Cu substrate where, if the Co grows fcc, single domain Cu overgrowth might be achievable. However, an insight into whether the growth on individual terraces is of two-domain type or has one of the domains either totally or partially suppressed would be provided if the adsorption site (either fcc, hcp or mixed) of the first Cu layer could be deduced and this will be discussed in more detail later.

The VEGAS simulations in Fig. 7 do not relate to an ideal fcc structure since it is known from Fig. 5 that a strain profile involving some rhombohedral stretching of the ideal lattice exists within the grown layer. In addition to the incorporation of the measured strain profiles, it was also necessary to take into account disorder in the grown films, which gives rise to in a reduction in the amplitudes of the observed blocking dips. This has been accomplished by mixing the simulation

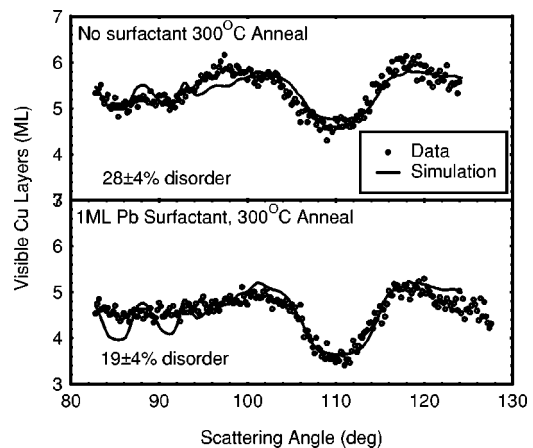


FIG. 7. VEGAS fits for the Cu overlayer signal for twinned fcc structure with strain profiles derived from Fig. 5 and additional intensity coming from disorder in the grown films. The Pb grown film clearly requires less disorder than its non-surfactant grown counterpart.

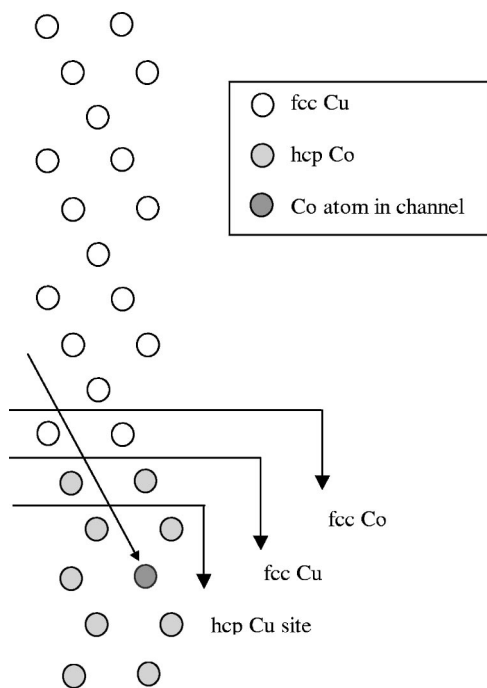


FIG. 8. Schematic representation of the model used to simulate the top two layers of Co signal using VEGAS. By varying the height of the two layer data extracted various structural models could be tested.

with flat signal typical of that expected for an amorphous target, a technique which has been used previously in the investigation of Co growth on Cu(111) (Ref. 3) and Au growth on Cu(111).¹³ The proportions of crystalline and amorphous material have been fitted using a χ^2 reliability factor following previous methodology.¹¹ The fits indicate greater disorder for the nonsurfactant grown sample ($28 \pm 4\%$) than that grown with Pb ($19 \pm 4\%$). The difference of $9 \pm 6\%$ in the degree of disorder shows a statistically significant improvement in crystallinity, confirming the qualitative improvement seen in the azimuthal channeling data.

VEGAS simulations have also been used to simulate the top two layers of Co signal, since this should reveal the adsorption site of the first layer of Cu and, if present, the existence of any fcc-like Co near the interface. Figure 8 shows a graphic representation of the model used to simulate the blocking spectrum expected from the first two Co layers. This model uses ten layers of fcc Cu above five layers of hcp Co. Simulated blocking spectra for hcp and fcc adsorption sites along with the top layer of Co being fcc can be produced from this single model by extracting the appropriate two layers as indicated in the diagram. Of course, for two of the three possibilities one of the extracted layers has the wrong atomic species present, but since the two elements are so close in atomic number this is unlikely to have a significant effect on the blocking curves produced. The three simulated blocking curves obtained are presented, along with a simulation for bulk hcp Co, in Fig. 9. The first observation from these curves is that all three geometric configurations approximately fit the major features of the experimental data

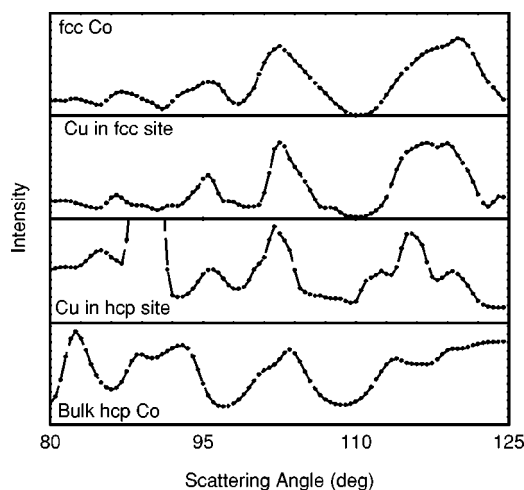


FIG. 9. VEGAS simulations of blocking curves for the top two Co layers beneath a 10-ML thin film of Cu with a bulk Co simulation for comparison. Note the similarity between the spectra produced for all three structural models.

(i.e. the two large dips at 99° and 111°) such that even in the case of an fcc-like Co layer the simulated spectrum looks quite similar to the hcp bulk. However, the data also contains two smaller dips at 119° and 123° (see Fig. 4), and while the first of these is only present for the Cu hcp site the second is only found in the Cu fcc site simulation. The data set also indicates no blocking dip at 91° where both the Cu fcc site and fcc Co simulation indicate that one should be present. In the Cu hcp site simulation a large spike in intensity is seen at this angle (going off scale as presented), which arises because the change in structure from fcc to hcp places a Co atom in the center of a channel (indicated on Fig. 8). Intensity spikes of this type have been observed experimentally in previous MEIS experiments¹⁶ but typically these effects are overestimated by VEGAS possibly because the focussing effects near the shadow cone edge are not well modeled. In addition, the presence of disorder in the overlayer and surface roughness would have the effect of smearing out this effect in angle and energy respectively. Hence it is possible that an effect of this type is responsible for “filling in” the blocking dip that would otherwise be expected at this angle. The most plausible explanation of the topmost Co layer data is that Cu atoms are adsorbed in both fcc and hcp sites above an entirely hcp Co substrate. However, bearing in mind the similarity of all the simulated blocking spectra in Fig. 9 the presence of some Co in an fcc-like configuration cannot be entirely ruled out.

The strain profiles shown in Fig. 5 indicate a further significant benefit in using Pb surfactant in the growth of the Cu layer, since an additional 1–2 ML have grown epitaxially. The reason for this extended epitaxy may be the reduction in the strain seen in the layers nearest the interface. Traditionally, the transition from two-dimensional Franck–van der Merwe (FM) growth to three-dimensional Volmer–Weber (VW) growth is governed by the following equation.¹⁷

$$\Delta E = E_{FV} - E_{VW} = (\gamma_o + \gamma_i)A - 1/2(\gamma_o + \gamma_i + \gamma_s)A,$$

where γ_s and γ_o are the surface energy per unit area A of the clean surface and the overlayer respectively and γ_i is the interfacial energy. The interfacial energy increases linearly with the strain energy and, hence, as the strain goes down the number of epitaxial layers should increase. In this work, the reduction in strain of the grown layer from 5.6% to 4.5% when using the Pb surfactant should give rise to a factor of 1.24 times the number of epitaxial layers or in other words for an initial number of 6 layers, an additional 1.5 layers should be allowed, in excellent agreement with the observed data.

The question still remains as to the mechanism by which the strain is relieved in the surfactant grown films. The compositional data in Fig. 3 demonstrated that a constant concentration of residual Pb was distributed throughout the grown film at a level of 5%, and in Fig. 6 it was shown that this residual Pb sits in the lattice sites. It is difficult to see how Pb atoms filling vacancies in an otherwise perfect Cu lattice could reduce the strain level, since a comparison of the metallic radii of the two elements shows Pb to be somewhat larger than Cu (1.750 Å as opposed to 1.278 Å). However, if the surfactant were present in some form of metal-vacancy cluster then it could potentially be space saving. In addition, one might imagine other more complex defects that could be induced by the presence of the Pb such that the strain properties were modified. If this were the mechanism by which strain was relieved then surfactant mediated growth could be viewed as a form of defect engineering, since clearly there are also defects present in the nonsurfactant grown films (as evidenced by the reduced crystallinity) but in that case not defects which improve the film properties. Previous studies of surfactant mediated growth have tended to ignore the residual surfactant even though it has been known for some time that the surface concentration depletes with increasing film thickness [e.g., Sb surfactant in the homoepitaxial growth of Ag(111) (Ref. 18)]. This may be because the techniques employed such as STM, AES, etc. are too surface specific to be able to probe the subsurface surfactant. Traditional theories of the action of the surfactant tend to emphasise the effects on adatom nucleation and mo-

bility during growth. However, while it is possible that factors such as these may contribute significantly to the effect, they are not parameters that have been probed in these experiments. In any case, further investigation of the potential contribution of residual surfactant in metal-on-metal growth systems would clearly be desirable.

One further issue that arises from Fig. 5 is the large surface contraction seen in the top 2–3 layers of the sample grown without surfactant. The fits to the energy curves shown in Fig. 3 incorporated some roughness in the deposited layer that was seen to be greater for the nonsurfactant grown sample than that grown with the surfactant. For a very rough surface a large proportion of the atoms will be found in effectively step-edge-like sites. Previous work on vicinal Cu surfaces using LEED (Ref. 19) and some theoretical calculations²⁰ have shown that step edge atoms exhibit large relaxations into the surface of approximately 8–10%, values which are broadly in line with the relaxation observed here.

V. CONCLUSIONS

Growth of Cu on a Co(0001) substrate led to the formation of thin films with a two-domain fcc structure. The use of a Pb surfactant had a beneficial effect on the growth, improving the crystallinity in the films and allowing more layers to grow epitaxially before the onset of three-dimensional growth. The increase in the number of epitaxial layers can be attributed to reduced strain in the grown films. Residual Pb at a constant level of 5% could be observed throughout the surfactant grown films. Annealing samples grown both with and without Pb surfactant to 300 °C was seen to have no effect on film properties.

ACKNOWLEDGMENTS

The FOM Institute in Amsterdam, Netherlands and Dr. P. D. Quinn, currently at the University of Potsdam, Germany, are acknowledged for provision of the VEGAS code and a revised front end, respectively. The SIMNRA code comes from the Max-Planck-Institut für Plasmaphysik, Garching. The Engineering and Physical Sciences Research Council is thanked for funding this work.

*Author to whom correspondence should be addressed. Email address: t.c.q.noakes@dl.ac.uk

¹M. A. Howson, *Contemp. Phys.* **35**, 347 (1994).

²J. Xu, B. J. Hickey, M. A. Howson, D. Grieg, M. J. Walker, and N. Wiser, *J. Magn. Mater.* **156**, 69 (1996).

³W. F. Egelhoff, Jr., P. J. Chen, C. J. Powell, M. D. Stiles, R. D. McMichael, C. L. Lin, J. M. Sivertsen, J. H. Judy, K. Takano, and A. E. Berkowitz, *J. Appl. Phys.* **80**, 5183 (1990).

⁴J. Camarero, T. Graf, J. J. de Miguel, R. Miranda, W. Kuch, M. Zharnikov, A. Dittschar, C. M. Schneider, and J. Kirschner, *Phys. Rev. Lett.* **76**, 4428 (1996).

⁵M. T. Butterfield, M. D. Crapper, T. C. Q. Noakes, P. Bailey, G. J. Jackson, and D. P. Woodruff, *Phys. Rev. B* **62**, 16984 (2000).

⁶M. T. Kief and W. F. Egelhoff, Jr., *Phys. Rev. B* **47**, 10785 (1993).

⁷J. de la Figuera, J. E. Prieto, G. Kostka, S. Muller, C. Ocal, R. Miranda, and K. Heinz, *Surf. Sci.* **349**, L139 (1996).

⁸J. E. Prieto, C. Rath, S. Muller, R. Miranda, and K. Heinz, *Surf. Sci.* **401**, 248 (1998).

⁹J. Camarero, J. de la Figuera, J. J. Miguel, R. Miranda, J. Alvarez, and S. Ferrer, *Surf. Sci.* **459**, 191 (2000).

¹⁰J. Camarero, J. Ferron, V. Cros, L. Gomez, A. L. Vazquez de Parga, J. M. Gallego, J. E. Prieto, J. J. de Miguel, and R. Miranda, *Phys. Rev. Lett.* **81**, 850 (1998).

¹¹P. Bailey, T. C. Q. Noakes, and D. P. Woodruff, *Surf. Sci.* **426**, 358 (1999).

¹²M. Mayer, 'SIMNRA Users Guide' Report IPP 9/113 (Max-Planck-Institut für Plasmaphysik, Garching, Germany, 1997).

¹³T. C. Q. Noakes and P. Bailey, *Thin Solid Films* **394**, 16 (2001).

¹⁴D. S. Gemmell, *Rev. Mod. Phys.* **46**, 129 (1974).

- ¹⁵J. F. Frenken, J. F. van der Veen, and R. M. Tromp, Nucl. Instrum. Methods Phys. Res. B **17**, 334 (1986).
- ¹⁶T. C. Q. Noakes, P. Bailey, P. K. Hucknall, K. Donovan, and M. A. Howson, Phys. Rev. B **58**, 4934 (1998).
- ¹⁷E. Bauer and J. H. van der Merwe, Phys. Rev. B **33**, 3657 (1986).
- ¹⁸H. A. van der Vegt, J. Vrijmoeth, R. J. Behm, and E. Vlieg, Phys. Rev. B **57**, 4127 (1998).
- ¹⁹S. Walter, H. Baier, M. Weinelt, K. Heinz, and T. Fauster, Phys. Rev. B **63**, 155407 (2001).
- ²⁰Z. J. Tian and T. S. Rahman, Phys. Rev. B **47**, 9751 (1993).